Thermochimica Acta, 174 (1991) 99–114
Elsevier Science Publishers B.V., Amsterdam

CHARGE DISTRIBUTION, PRESSURE AND COMPOSITION EFFECTS OF CuO_x BASED SUPERCONDUCTORS

J. ŠESTÁK, J. KAMARÁD, P. HOLBA, A. TŘÍSKA, E. POLLERT and M. NEVŘIVA

Institute of Physics of the Czechoslovak Academy of Sciences, Na Slovance 2, 18040 Praha 8 (Czechoslovakia)

(Received 20 August 1989)

ABSTRACT

Charge distribution on copper and associated forms of oxygen anions are discussed. Pressure effects on T_c are surveyed for various YBCO, BSCO and TBCO superconductors. Pseudobinary and quasiternary $YO_{1.5}$–BaO–CuO_x phase diagrams are reviewed including pseudobinary cuts between $YBa_2Cu_3O_x$, Y_2BaCuO_5, $BaCuO_2$ and $YCuO_{2.5}$.

INTRODUCTION

Superconductivity in copper oxide compounds has been found when their structures contain CuO_2 sheets with a single bridging oxygen within the sheets having 180° Cu–O–Cu linkages where a Cu–O subarray is oxidized beyond the formal copper valence Cu^{2+} [1–3]. The relevant structures are closely related to the perovskite, being remarkable for the low dimensionality of the copper–oxygen framework. Moreover, these oxides are characterized by a lack of oxygen stoichiometry, i.e. by variable Cu^{3+} content. For example, stoichiometric La_2CuO_4 and $YBa_2Cu_3O_6$ have copper in the formal valences Cu^{2+} and Cu^{1+} and are semiconductors. For $y > 0.05$ both the $La_{2-y}Sr_yCuO_4$ (LSCO) and $YBa_2Cu_3O_{6.5+y}$ (YBCO) become superconductors. In the latter system the Cu–O arrays are gradually oxidized beyond the formal copper valence 2+. Similarly, the $Bi_2(Sr, Ca)_3Cu_2O_8$ (BSCO) and $Tl_2Ba_2Ca_{n-1}Cu_nO_{4+2n}$ ($n = 1, 2, 3$; TBCO) exhibit CuO_2 layers oxidized beyond the formal valence $(CuO_2)^{2-}$ containing CuO_2 sheets with Cu–O–Cu interactions of almost 180°.

In many cases, however, it is not yet clear which compounds and phase boundaries are stable or metastable, owing to the complexity of reactions involved. With regard to the newer BSCO system we have much less information available; in particular, there is an absence of associated phase diagrams. An equally interesting point is the pressure dependence of the critical parameters; this usually falls outside major interests although the

0040-6031/91/$03.50

pressure effects certainly help to test the concept of hole superconductivity resulting from the analysis of charge distribution. The purpose of this article is to review charge distribution, pressure and composition effects within the framework of our results.

CHARGE DISTRIBUTION EFFECTS

The superconductivity of $YBa_2Cu_3O_x$ (1 : 2 : 3) is very remarkable because oxygen is removed by heating when the material converts from the superconducting ($x > 6.5$) to the non-superconducting ($x < 6.5$) structure without a collapse of its general network. This is appropriate to the reduction of the formal copper valence Cu^{m+} as follows [4]:

$$m+ = (6 + 2y)/3 \quad \text{and} \quad Cu^{3+}/Cu^{2+} = 2y/(3 - 2y) \quad (\text{if } x = 6.5 + y)$$

and was repeatedly investigated by weight measurements (for thermogravimetric data see e.g. ref. 5). This behaviour can also be explained by the existence of a local intergrowth of two structures [3], i.e. regions characterized by a modulation involving a doubling of their a lattice parameter in agreement with the stacking of one $(CuO_2)^{1-}$ superconductive array with one $(CuO)^{1-}$ metal-like row. More complex reactions involved in oxidation were discriminated on the basis of emanation thermal analysis (ETA) [6] showing two simultaneous but distinct processes of oxygen intake and ordering.

The disproportionation [7] becomes crucial to the appearance of high-temperature superconductivity (HTS) and is largely governed by the relative ionization potentials and electron affinities for the three charge states concerned. The YBCO charge distribution can be written as follows:

$$Cu^{2+}(d^9) \rightarrow Cu^{3+}(d^8) + e^-$$

or in terms of bridging (O^{2-}) half-bridging (O^-) and non-bridging (O^0) oxygens as e.g.

$$Cu^{3+}(d^8) + O^{2-}(p^6) \rightarrow Cu^{2+}(d^9) + O^-(p^5) \text{ or even } \tfrac{1}{2}(O_2)^{2-}$$

(as originally developed for magnetic systems of oxides [8] and glasses [9]). It is worth noting that similar behaviour can be expected for nickel ions, as shown by a simplified energetic scheme [2,7] for binary oxides of the $3d$ series. This could be accomplished by a mutual positioning of the oxygen band and d levels if suitably adjusted using appropriate Ni-based structures and compositions. Recently, however, vanadium ions were shown to be of a more perspective applicability.

Methods such as X-ray excited Auger spectroscopy and X-ray photoelectron spectroscopy (XPS) were employed to prove the existence of Cu^{3+} ions [3,7,10–12]. The XPS measurements of Pollert et al. [7] showed a large overlap of the oxygen s, p states and copper d states of the 1 : 2 : 3 structure

in comparison with Cu_2O and CuO and the presence of peroxidic anions was detected by several techniques including polarography [13]. In order to obtain further information XPS [3,7,10] was utilized. In the superconducting 1 : 2 : 3 ($X < 6.9$) only negligible *a*-axis oxygen is present to provide the O–O contact required for hole trapping at a peroxide ion. Where $x > 7$ definite *a*-axis oxygen makes direct O–O contacts with neighbouring *b*-axis oxygen within Cu(1) planes, as for example the tetragonal semiconductor $LaBa_{1.5}La_{0.5}Cu_3O_{7.19}$ [3]. Both samples showed a peak at about 531 eV that is apparently assigned with surface species (e.g. oxygen associated with carbon or hydrogen). Qiu et al. [12] identified this peak with a surface hydroxyl species similar to that found in low temperature water adsorption on transition metal studies. While molecular water desorbed during the heating of 1 : 2 : 3 to room temperature exhibited a peak at 534 eV, Ford et al. [11] found that in the evacuated sample heated to 450 °C the 531 eV peak was reduced by about 60% and regained its original intensity when consequently exposed to atmosphere. They concluded [11] that the oxygen initially removed by heating must derive from chemisorption active sites at the interfaces although no additional surface enhancement of the oxygen (O1*s*) or barium (Ba4*d*) peaks were noticed. However, they did not find the origin of a very weak third peak (O1*s*) at about 533 eV (existing at temperatures too high to be due to molecular water, as in ref. 12) which was not distinguished in the early study by Goodenough et al. [1] upon investigation of different 1 : 2 : 3 structures.

Since it is difficult to resolve the contributions from the different bulk anions one cannot distinguish the mutual contributions of monomers O^- or dimers $(O_2)^{2-}$ to the peak observed at about 533.5 eV (see Fig. 1). Assuming the redox reaction in the 1 : 2 : 3 structure takes place readily in the basal Cu(1) plane one can assume the formation of oxygen holes in the vicinity of $[Cu(1)O_3]^{m+}$ layers. Owing to the large distance between the Cu(2) and O(1) [7] and following a relatively weak overlap of d_{z^2}(Cu(2)) and p_6(O(1)) orbitals the monomeric holes can probably be attached to the apical oxygens O(1). Besides basic thermodynamic conditions are assumed, the formation of peroxidic anions $(O_2)^{2-}$ in the superconducting 1 : 2 : 3 requires, at the same time, a suitable geometric arrangement of oxygen anion linkage between *a*-axis and neighbouring *b*-axis oxygen in the Cu(1) plane. It seems that twin walls make possible the dimerization of oxygen anions. A comparable concentration of peroxidic anions, yielded by our polarographic analysis [13] and the densities of 'states' calculated from the twin boundary distances, which makes possible the formation of pairs $(O_2)^{2-}$, is in the order of 10^{20} cm^{-3}, indicating that the possibility of peroxidic anion formation at room temperature is very small. For the semiconductor 1 : 2 : 3 with $x > 7.0$ [1] the formation of $(O_2)^{2-}$ is expected owing to the disordered and excess oxygen. The O(1*s*) binding energy of dimeric peroxide ions lies between that of bridging oxygen ions O^{2-} and half-bridging O^-, and

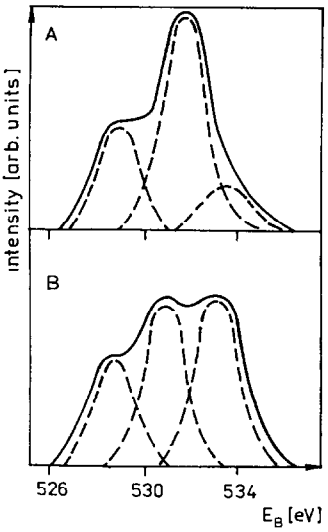

Fig. 1. Typical O ($s1$) XPS spectra [1,7] (intensity vs. binding energy) measured at T about 80 K for two characteristic states: (A) superconducting orthorhombic 1:2:3 ($T_c \approx 90$ K and $x \approx 6.9$) exhibiting well-resolved peaks at about 531 and 529 eV; (B) semiconducting tetragonal 1:2:3 ($x \approx 7.2$ where Y and Ba are partly substituted by La) exhibiting the third well-resolved peak at about 533 eV.

trapping out of the O($2p$) holes at dimeric species supports [1] the splitting of the bulk oxygen peak into two well-resolved peaks, cf. Fig. 1. Goodenough et al. [1] suggested that for a given system T_c appears to increase initially with the concentration of mobile excess holes until these holes become trapped, the trap states being primarily of $(O_2)^{2-}$ character.

A redistribution of the charge density below T_c leads to the formation of additional monomeric oxygen holes

$$Cu^+(d^9) + O^{2-}(p^6) \rightarrow Cu^+(d^{10}) + O^-(p^5)$$

Once a critical density is exceeded, the occupation of $[Cu(2)O_2]^{2-}$ planes becomes energetically more favourable and one can suppose that holes are transferred from the chains into the pyramidal planes. Thus it seems that $[Cu(1)O_3]^{m+}$ layers in $YBa_2Cu_3O_{7-x}$, and probably also Bi–O or Tl–O layers in the respective superconductors, play an essential role as a charge reservoir controlling the conductivity mechanism in the $[Cu(2)O_2]_n$ planes.

The question of oxygen distribution and content in BSCO and TBCO has not yet been elucidated and is still of essential importance for a better understanding of their superconductivity. It was confirmed that the intergrowth between the distorted rock salt-type layers and the oxygen-deficient perovskite layers are potentially the most suitable structures for new superconducting materials as developed less recently with LSCO. It is worth noting that the 80 K superconductor $Bi_2Sr_2CaCu_2O_{8+y}$ and the 110 K superconductor $Tl_2Ba_2CaCu_2O_{8+y}$ have very similar structures (the only

difference being in the distances between Bi and Tl planes). The critical temperatures are dependent on the frequency and multiplicity of the superconducting $(CuO_2)^{1-}$ layers which encourages one to attempt syntheses of YBCO, BSCO and TBCO with an increased thickness of the perovskite layers predicted [14,15] to exist possibly as metastable compounds [15]. Some of these compounds have already been discovered as the YBCO double-layered 1 : 2 : 4 [16] or 1 : 2 : 3.5 [17] with semiregular frequency of the double layers.

PRESSURE EFFECTS

Increased pressure may destroy the superconducting contacts in the ceramic materials [18] but for the entire 1 : 2 : 3 structure the pure hydrostatic pressure raises the T_c and improves conductivity above T_c [19]. Presumably, the increased p/d overlap screens out the disorder scattering. In the first generation of LSCO and LBCO superconductors ($T_c \approx 40$ K; tetragonal crystal structure), Dietrich et al. [20] and Schirber et al. [21] presented values similar to those obtained by Chu et al. [22], who first observed the large and positive increase in T_c with pressure at a rate of about 9 K GPa^{-1} giving pressure parameters $dT_c/dp = 2.95$ and 3.5 K GPa^{-1}, respectively. In contrast, the next generation of HTS YBCO, BSCO and TBCO compounds ($T_c = 90$–120 K; orthorhombic crystal structures) have exhibited only moderate shifts of T_c with pressure with $dT_c/dp \leqslant 2$ K GPa^{-1} [19,21,23–25]. From this point of view, the ceramic superconductors can be divided into two groups with strong and moderate sensitivity of T_c to pressure. This different pressure response cannot be explained by the different compressibilities of the compounds. All the presented values of their bulk modulus B are within a narrow range around $B = 170$ GPa [20,26–28]. However, the effect of pressure on the lattice constants is different in the compounds investigated. X-ray pressure studies have indicated isotropic compression of the crystal lattice in the tetragonal LSCO compounds with $d \ln a/dp = d \ln c/dp = -2.5 \times 10^{-3}$ GPa^{-1} [26] and anisotropic compression of the orthorhombic YBaCuO compound [27,28] giving two possible interpretations of the experimental results:

$$d \ln c/dp = -2.32 \times 10^{-3} \text{ GPa}^{-1}$$

and

$$d \ln a/dp = d \ln b/dp = -1.71 \times 10^{-3} \text{ GPa}^{-1}$$

or

$$d \ln b/dp = -2.39 \times 10^{-3} \text{ GPa}^{-1}$$

and

$$d \ln c/dp = d \ln a/dp = -1.66 \times 10^{-3} \text{ GPa}^{-1} \quad [27].$$

The second version seems to reflect the different occupation of the oxygen

TABLE 1

Critical temperatures of the ceramic superconductors and their pressure derivatives

Sample	T_c (K)	dT_c/dp (K GPa^{-1})	F [a]	Ref.
$Ba_{1-x}K_xBiO_3$	16	$+1.0\pm0.2$	−10.6	21
	23	$+0.8\pm0.2$	−5.9	21
$La_{1.8}Ba_{0.2}CuO_4$	32	+9	−48	22
$La_{1.8}Sr_{0.2}CuO_4$	33	+2.95	−15.2	20
$La_{1.85}Sr_{0.15}CuO_4$	39	$+3.5\pm0.5$	−15.2	21
$YBa_2Cu_3O_{7-x}$	92	+0.7	−1.3	25
	90	+0.9	−1.7	23
	92.5	$+1.1\pm0.1$	−2.0	18
	95	+1.3 [b]	2.3	24
$GdBa_2Cu_3O_{7-x}$	94	+1.3	−2.3	23
$ErBa_2Cu_3O_{7-x}$	91	+1.4	−2.6	23
$YbBa_2Cu_3O_{7-x}$	88	+1.9	−3.7	23
$EuBa_2Cu_3O_{7-x}$ orth.	90	+1.6	−3.0	32
tetra.	60	+9	−25	32
BiSrCaCuO	109.5	$+3.2\pm0.8$	−5.0	38
	87	$+1.4\pm0.1$	−2.7	38
	108	$+1.6\pm0.5$	−2.5	21
	85	$+2.4\pm0.2$	−4.9	21
(BiPb)(SrCa)CuO	106.5	$+2.3\pm0.2$	−3.7	36
	70.5	$+1.0\pm0.3$	−2.4	36
TlBaCaCuO	106	$+2.0\pm0.4$	−3.2	21
	114	+2.1	−3.1	39

[a] $F = d\ln T_c/d\ln V = -(B/T_c)\cdot dT_c/dp$, where $B = 170$ GPa.
[b] Up to 15 GPa.

positions in the a and b axes and it is supported by the observed transition from orthorhombic to tetragonal phase in EuBCO under a pressure of 20 GPa [29]. Neutron diffraction measurements [30], which gave the strongest decrease in the c lattice constants and the smallest decrease in the b lattice constants under cooling in the orthorhombic YBCO compound, seem to support the first version. Estimation of the upper limit of dT_c/dp of the YBCO superconductor, based on thermal expansion measurements [31], gave the value $dT_c/dp = +1.3$ K GPa^{-1}, surprisingly comparable with experiments [19,21,23,24] (see Table 1).

The tetragonal phases of the REBCO superconductors were prepared [25,32] by 3-d metal (Fe, Co) substitution or by temperature treatment of EuBCO in vacuum, i.e. by oxygen losses. The critical temperatures T_c of tetragonal phases prepared in this way were substantially lower and the compressibility of the tetragonal YBCO was higher [28] in comparison with their orthorhombic counterparts. In addition, the tetragonal phases showed a pressure parameter dT_c/dp which was much greater than that of the orthorhombic phases [25,32]. The effect of the sample oxygen deficiency on their dT_c/dp seems to be at least as important [25] as the structural aspect.

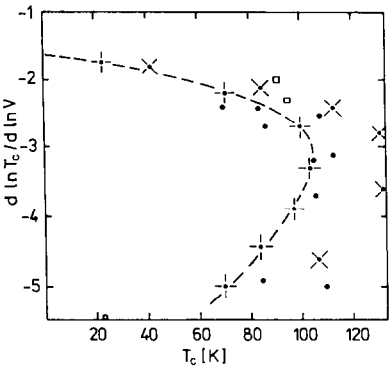

Fig. 2. Fit of the theoretical relations on the experimental data: □ (Y or RE)BaCuO; ●, BiSrCaCuO and TlBaCaCuO; ○, BaKBiO; (— — —) theory with $U = 5$ eV, $t = 0.35$ eV, $\mathrm{d} \ln t / \mathrm{d} \ln V = -5/3$.

The pressure coefficients $F = \mathrm{d} \ln T_c / \mathrm{d} \ln V$ of the superconducting oxide compounds studied were discussed [33,34] within Cyrot's model [35] of high T_c superconductivity. The critical temperature T_c is given within this model by the BCS-like formula

$$T_c = t\delta \exp(-\delta U/t)$$

and the pressure coefficient F can be derived under the assumption $\mathrm{d} \ln U / \mathrm{d} \ln V = 0$ as

$$\mathrm{d} \ln T_c / \mathrm{d} \ln V = -(B/T_c)\, \mathrm{d}T_c/\mathrm{d}p = \mathrm{d} \ln t / \mathrm{d} \ln V (1 + \delta U/t)$$

where t is the hopping integral, proportional to the width W of the d energy band, U is the intra-atomic Coulomb repulsion energy and δ is the average number of holes in the energy band which are introduced by the Cu^{3+} ions. The volume dependence of t was estimated by Heine's formula $\mathrm{d} \ln t / \mathrm{d} \ln V = \mathrm{d} \ln W / \mathrm{d} \ln V = -5/3$ (see e.g. ref. 34). The critical temperature T_c reaches its maximum at $\delta = t/U$ and the positive value of $\mathrm{d}T_c/\mathrm{d}p$ increases with increasing hole concentration δ. Using $U = 5$ eV, the value $t = 0.35$ eV was obtained by the fit of the theoretical relations on the experimental data given as the pressure coefficient F vs. T_c plot in Fig. 2 [36].

The high values of the pressure parameter $\mathrm{d}T_c/\mathrm{d}p$ of the tetragonal LBCO and LSCO superconductors could be described within this model only by an unrealistically high concentration of holes. Similarly, the decrease in T_c and the simultaneous increase in $\mathrm{d}T_c/\mathrm{d}p$ caused by the oxygen deficiency in the tetragonal (Y or RE)BCO compounds cannot be explained by the increase in the hole concentration. Recently, the similar positive values of $\mathrm{d}T_c/\mathrm{d}p$ have been observed in the cubic $Ba_{1-x}K_xBiO_3$ superconductor [21], where the absence of the d-metals turns attention back to the basic question of the mechanism of high T_c superconductivity.

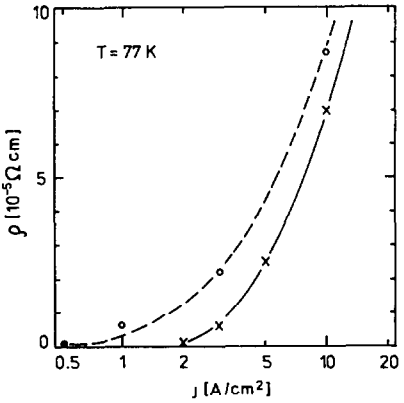

Fig. 3. Dependence of the resistivity of (BiPb)(SrCa)CuO on the measuring current density at 77 K under normal pressure (———) and at 0.3 GPa (— — —).

In comparison with the conventional superconductors, much lower critical current densities have been observed in polycrystalline ceramic superconductors. A comparison of the temperature dependences of resistivity and a.c. susceptibility of ceramic superconductors [37] leads to the conclusion that separated grains become superconductive when transition to the superconducting state begins. A heterogeneous intergrain material, a structural mismatch and the short coherence length resist the passage of the supercurrent between the superconducting grains up to the temperature at which the connectivity is established via weak junctions. These weak junctions are very sensitive to the conditions of the sample preparation and to the external fields [36]. The effect of the measuring current on the resistivity of the (BiPb)(SrCa)CuO superconductor was measured at 77 K under normal and elevated pressures [36]; the results are plotted in Fig. 3. The weak junctions became resistive at the lower current density when the higher pressure was applied. Under hydrostatic pressure, the decrease of the critical current density was reversible.

COMPOSITION EFFECTS

Despite an intensive HTS investigation, the phase relations are still far from being fully understood although the basic approach does require the identification of compounds and the determination of relevant phase boundaries (see e.g. refs. 15, 40, 41). High temperature superconductivity is caused by the inherent heterogeneity of materials mostly prepared by ceramic routes which involves the creation of grain surfaces assumed to be different from the property of the bulk (e.g. difficulty in preparing single phased BSCO materials owing to the phase separation probably induced by interface curvature). In addition, the unwanted formation of intermediate

compounds (usually enhanced by inhomogeneous mixing of components) and the separation of off-stoichiometric phases (initiated by parasite reactions with the surrounding atmosphere [40] or sample holders [15]) is a frequent source of ambiguous data.

The starting information is conveniently provided by binary phase diagrams recently surveyed by Šesták [15], Roth et al. [40] and Nevřiva [41]. The phase diagram of the Cu–O system was proposed less recently [42] using thermal, dissociation and microscopic data of a number of previous authors. CuO and Cu_2O were indicated as phases of fixed composition with negligible departures from stoichiometry. These oxides form eutectics at about 13 wt.% oxygen corresponding to about 68 mol% Cu_2O and melt at 1075 °C. Under oxygen pressure of 1 atm, melting of heated CuO occurs at about 1110 °C and is accompanied by loss of oxygen and formation of an oxygen-deficient liquid phase (slag). With further temperature increase the loss of oxygen becomes more progressive and at about 1400 °C a saturated solution of oxygen in liquid copper is formed. In air, Cu_2O is formed at about 1020 °C, followed by melting at about 1120 °C to produce the liquid metal. The dissociation curves and melting temperatures of CuO were determined by Gadalla et al. [43].

Holba et al. [44] discussed the role of oxygen as a free component distinguishing between the conveniently closed Y–Ba–Cu–O and partly open Y–Ba–Cu–(O) systems. In addition to the classical description one more equation is valid in the latter case; this expresses the equality between the oxygen chemical potentials of the surrounding (hopefully controlled) atmosphere and that of the condensed phases in question. As a consequence, the number of degrees of freedom is reduced by one so that the usual form of phase ruling applies as if the system consisted only of the fixed non-volatile components. The concentration of fixed components must then be presented in quantities which are independent of the actual content of the free component (oxygen). Following this concept and accounting for the knowledge of double-oxide phases the expected phase relations in the Me_1–Me_2–O systems can be suggested in the form of quasibinary (x–T) diagrams, as illustrated in Fig. 4. It is worth noting that with increasing temperature the stability of oxygen-poor solid phases can increase while the stability of oxygen-rich melts decreases; this may result in solidification on heating and in melting upon cooling of the samples of given composition. Owing to the existence of two or three partly immiscible melts, more than one liquidus curve can be observed, cf. Fig. 4. These as yet neglected phenomena can disrupt the conventional procedures of phase equilibria investigations. The experimentally resolved CuO-rich parts of the series of quasibinary phase diagrams are shown in the cumulative form in Fig. 5 [15,40,44,45,48,51].

It is obvious that in addition to the relevant YBCO phase diagrams the corresponding quasibinary relations for BSCO and TBCO are equally neces-

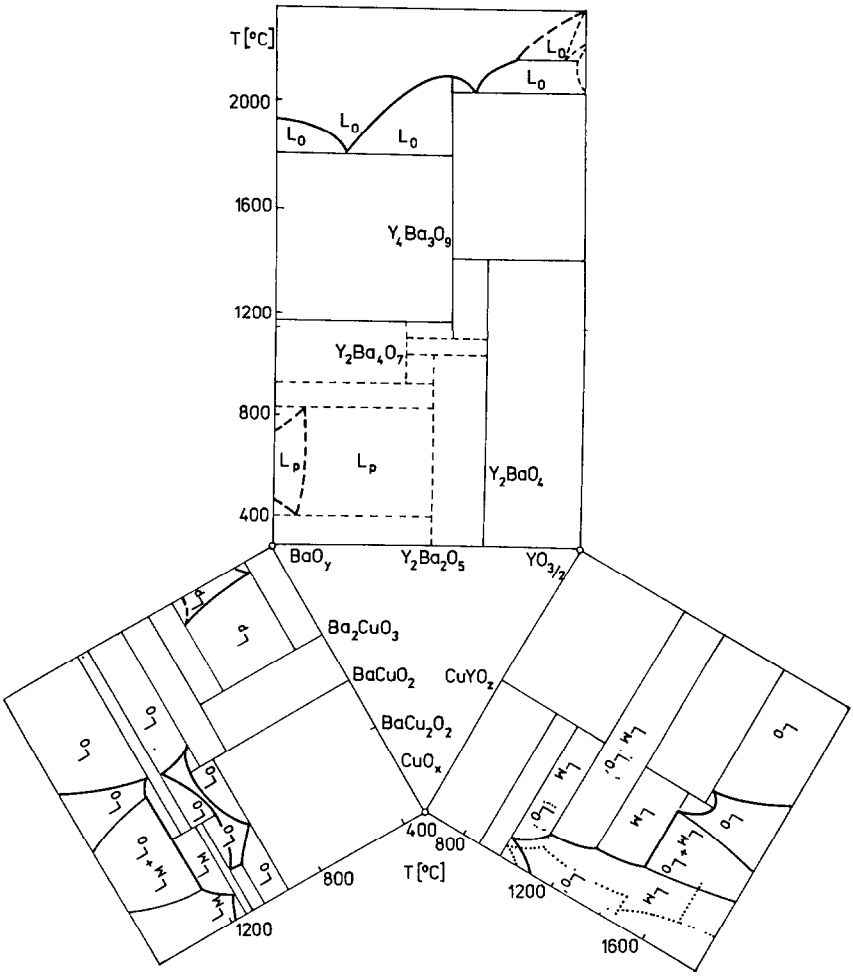

Fig. 4. Expected $x \sim T$ diagrams [44] of Cu–Y–(O), Cu–Ba–(O) and Y–Ba–(O) systems in air. Bold solid lines show the liquidus and dashed lines indicate metastability. The bold dotted line shows the shift of the boundaries in oxygen. Three different types of melt are marked as L_M, L_O and L_P to describe metallic melt, oxide melt (slag of mainly $BaO + CuO_x$) and peroxide melt (mainly BaO_2), respectively.

sary. However, the basic data here are still missing, the only data available are those for the Bi_2O_3–CaO [46] and Bi_2O_3–SrO [47] binaries jointly treated in [59].

Accordingly, the ternary phase diagrams were proposed to include variability of copper oxide states [48–57]. A convenient approach seems be the four-dimensional representation of the CuO–CuO_x–BaO–Y_2O_3 system depending on CuO_x [52,53]. Data reported by Przyluski et al. [52] are given in Fig. 6, showing the existence of various compounds (the formation of which was already questioned by De Leeuw et al. [58], Roth et al. [40] and Šesták [15]). In practice they used [52] prereacted samples representing the stable

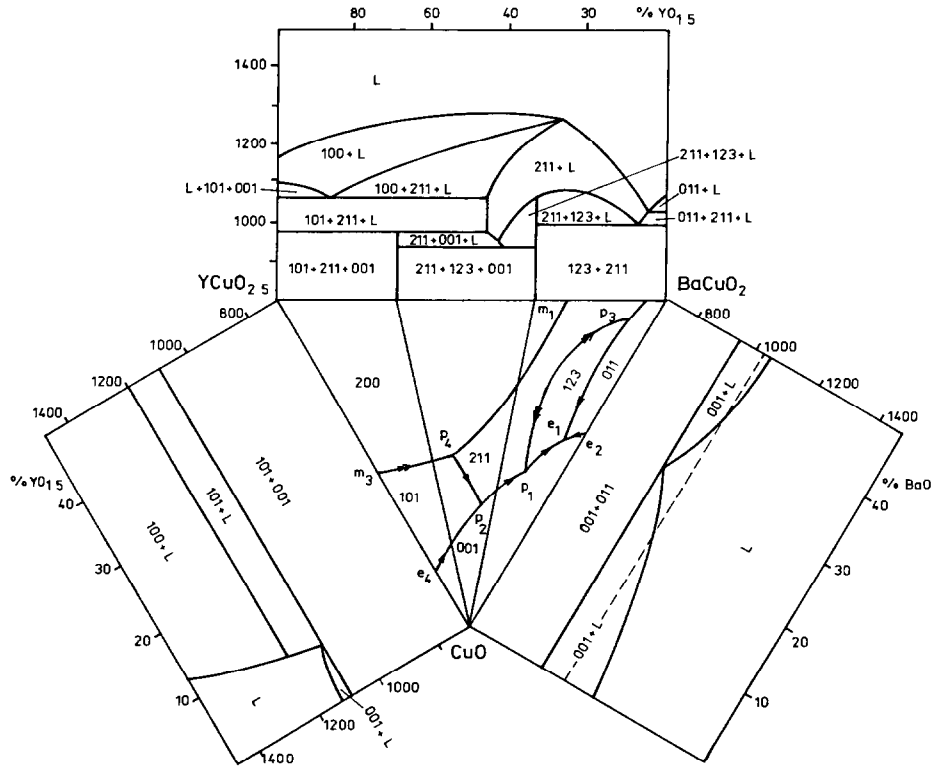

Fig. 5. Experimentally determined pseudobinary cut $YCuO_{2.5}$–$BaCuO_2$ in oxygen based on data from ref. 48 and corrected according to refs. 44 and 51, added by the oxygen determined x–T diagrams of $CuYO_{2.5}$–CuO and $BaCuO_2$–CuO [45]. Slightly modified liquidus surfaces derived from ref. 51 are inserted in the middle triangle: numbers (e.g. 1 : 2 : 3) give the ratio of Y : Ba : Cu; m, e and p are melting, eutectic and peritectic points to reach approximate values $p_1 = 940$, $p_2 = 975$, $p_3 = 1000$, $e_1 = 890$, $e_2 = 920$, $e_4 = 1110$ and $m_3 = 1120\,^\circ C$.

phase combination existing in air and mixed them with Cu_2O and annealed in evacuated silica tubes at 950 °C for 50 h. After quenching, the sample composition was analysed by XRD and the EMF values were measured in the range 750–1000 °C. For the presentation of possible non-stoichiometry of the triple oxides in air at 950 °C the tetrahedron was used [52], cf. Fig. 6, where 1 : 2 : 3 ($YBa_2Cu_3O_{6.02}$), 1 : 4 : 3 ($YBa_4Cu_3O_{8.01}$), 3 : 8 : 5 ($Y_3Ba_8Cu_5O_{16.45}$) and 1 : 5 : 2 ($YBa_5Cu_2O_{8.35}$) phases were distinguished. For the copper partial reduction in the different oxides with a given Y : Ba : Cu ratio the composition moves along lines drawn through the existence points on the two planes $YO_{1.5}$–BaO–CuO and $YO_{1.5}$–BaO–$CuO_{0.5}$, the latter indicating the complete reduction of Cu^{2+} to Cu^{1+}. Consequent oxidation upon slow cooling gradually shifts the oxide composition along the lines which can be drawn through the two points on these two planes, the $YO_{1.5}$–BaO–$CuO_{1.5}$ one showing maximum Cu^{3+} content. The oxygen content of these four phases increased to the following values: 1 : 2 : 3 (6.98), 1 : 4 : 3 (8.97), 3 : 8 : 5 (18) and 1 : 5 : 2 (8.97). From the measured oxygen potentials the

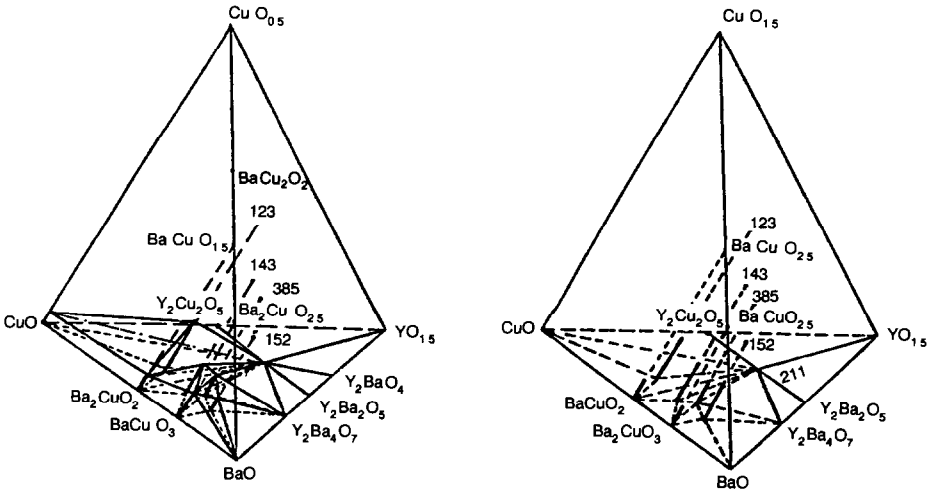

Fig. 6. Left, the $CuO-YO_{1.5}-BaO-CuO_{0.5}$ system equilibrated in air at 950 °C [52]; right, the corresponding non-stoichiometry developed by oxidation of the former system when cooled slowly in air to room temperature. Gibbs energies (in J) of solid-state reactions yielding the above-mentioned ternary phases as determined by EMF measurements are (from ref. 52): $Y_2Ba_2O_5 + Y_2Cu_2O_5 = 2(2:1:1)$ $(-2311 - 16.3\ T)$; $Y_2O_3 + 2CuO + Y_2Ba_2O_5 = 2(2:1:1)$ $(6799 - 30.5\ T)$; $Y_2O_3 + Y_2Ba_2O_5 + 14BaCuO_2 = 4(1:4:3) + 2CuO$ $(-2180 - 24.3\ T)$; $Y_2O_3 + 6CuO + Y_2Ba_2O_5 + 6BaCuO_2 = 4(1:2:3)$ $(13820 - 37.5\ T)$; $4Y_2O_3 + 4Y_2Ba_2O_5 + 13(1:4:3) = (2:1:1) + 7(3:8:5)$ $(-14920 - 93.6\ T)$; $2Y_2BaO_4 + 7BaCuO_2 = (1:2:3) + 2(1:4:3)$ $(-188300 + 142.5\ T)$; $Y_2BaO_4 + 3BaCuO_2 + 3CuO = 2(1:2:3)$ $(-88395 + 66.2\ T)$.

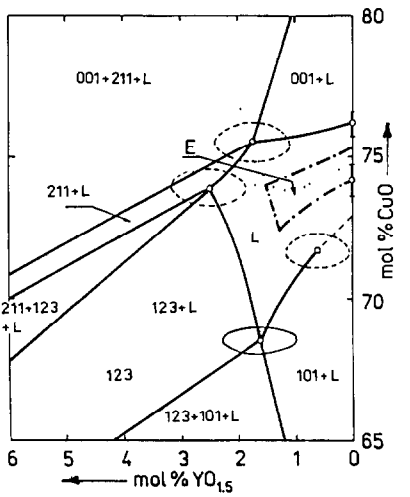

Fig. 7. Isothermal cut of the $CuO-BaCuO_2-YBa_2Cu_3O_x$ pseudoternary system at 975 °C in oxygen [41,44,50]. The ternary eutectic point (E) was estimated to be at about 75.2 mol% CuO and 1 mol% $YO_{1.5}$. Uncertainties in the individual melt compositions are expressed by the solid and dashed elipses, the axes of which correspond approximately to the deviations calculated in ref. 50).

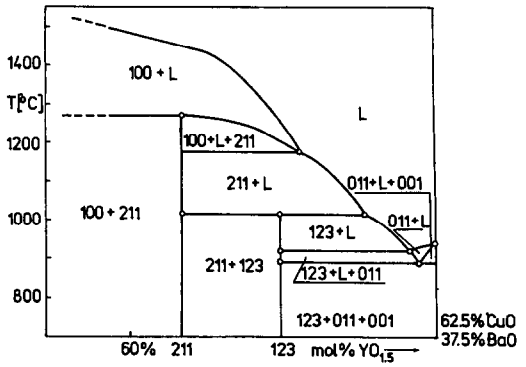

Fig. 8. Pseudobinary cut containing the stable 2:1:1 and 1:2:3 phases as derived according to ref. 44 on the basis of data in ref. 51 assuming the contradictory representations published in refs. 15, 40 and 54–57.

Gibbs energies were calculated (cf. Fig. 6 caption) and positive reaction entropies were discussed in terms of the plausible metastability of compounds [52].

An increasing number of studies was devoted to investigation of the pseudoternary Y–Ba–Cu–O system, but usually under conditions which do not guarantee the required content of oxygen. The equilibrium phase relations at the constant predetermined $p(O_2)$ can be represented by a triangle with the fixed components at the corners only if the barycentric coordinates are chosen to be independent of the real oxygen content. From the point of view of single crystal growth the most interesting diagrams were reported by Oka et al. [49] and Scheel and Licci [57] who assembled the area along the four directions starting from the 1:2:3 phase towards CuO, $Ba_3Cu_{12}O_{15}$, $Ba_3Cu_7O_{10}$ and $Ba_3Cu_5O_8$. The phase relations in the system CuO–O:1:1–1:2:3 at 950 °C in oxygen were determined by Nevřiva et al. [50] using a procedure based on the separation of the melt from an equilibrated sample and subsequent analysis of the solid residue. The resulting cut with approximate liquidus curves and boundaries of the four primary crystallization fields is shown in Fig. 7. Aselage and Keefer [51] determined phase relations in the CuO-rich corner of the $YO_{1.5}$–BaO–CuO ternary which is included in the middle triangle of Fig. 5. The $YCuO_{2.5}$–$BaCuO_2$ tie-line is one of the most intensively studied cuts [15,40,41,44,48,54,57] because it includes the superconducting 1:2:3 phase (see Fig. 5). Another very interesting cut is that between $YBa_2Cu_3O_x$ and Y_2BaCuO_5 [15,40,44,51,56,57] which is shown in Fig. 8.

CONCLUDING REMARKS

The presence of Cu^{3+} ions in the copper oxide compounds is held as a necessary precondition for superconductivity in these materials. The relevant

knowledge of the charge distribution in dependence on the oxygen content in YBCO and the large overlap of the oxygen s, p states and the copper d states [7] is compatible with the demonstrable pressure increase of the width of the d-energy band. It is also well known that the energy of d states of each element increases more slowly with decreasing volume than the energy of s, p states. Therefore, the large compressibility and the pressure sensitivity of T_c of the LSCO and LBCO superconductors (with tetragonal crystal structure) seems to reflect the more d-like character of the charge carriers in these compounds in comparison with the new generation of YBCO, BSCO and TBCO materials, where the p states in the overlapping (s, p, d) bands can play a more important role. Despite the anisotropic compressibility of all superconductors with orthorhombic crystal structure, we can assume a pressure effect on the formation and distribution of peroxidic $(O_2)^{2-}$ anions and their hole trapping mechanism.

The effect of pressure on the critical currents of the ceramic superconductors leads to an increase in the width and to changes in the shape of the resistive transition even if the pressure is hydrostatic. Therefore, the shifts of T_c with pressure discussed above must be carefully determined. Under quasihydrostatic pressures the intergrain junctions are destroyed and the temperature dependence of the resistivity of the ceramic superconductors exhibits a semiconductive character at temperatures above T_c. In this case the effect of pressure on the resistive junctions is observed but pressure does not seem to affect the critical temperature of the superconductive phase. The hydrostatic pressure and well-determined properties of the one-phase (if possible) samples seem to be the basic experimental conditions under which the important pressure parameters of the high T_c superconductors can be obtained and compared with the estimations of the relevant theoretical models.

The metastability of ternary compounds (cf. Fig. 6) and their possible existence in the form of oxycarbonates [15,40,58] and the mutual inconsistency of some reported phase boundaries [54] accounts for:

(i) contamination products effecting uncontrolled changes in the melt composition (e.g. the formation of Pt-substituted phases [15]);

(ii) the reverse reactions of BaO with CO_2 (which is always present even in very pure gases) resulting in the formation of $BaCO_3$, resulting in the distortion of the melt composition (saturation temperature) as well as the violation of standard phase ruling by adding an extra component (CO_2) [40]. It was found that $BaCO_3$ can be formed during most experiments carried out in air even above 900 °C if the thermodynamic inequality [50]

$$\log a_{BaO} + \log p(CO_2) > -3.0$$

is fulfilled (a_{BaO} and $p(CO_2)$ being the activity of oxide in the melt and partial pressure of carbon dioxide, respectively);

(iii) non-equilibrium interactions between the sample and oxygen affecting the total oxygen content and the phase compatibilities;

(iv) metastability of phases [15,44] obtained as a result of uncontrolled treatments, particularly to insufficient freeze-in of high-temperature states during quenching.

REFERENCES

1 J.B. Goodenough, A. Manthiram, Y. Dal and A. Campion, Supercon. Sci. Tech., 1 (1988) 187.
2 J.A. Wilson, J. Phys. C, 71 (1988) 2067.
3 B. Raveau, C. Michel, M. Hervien and J. Provost, Rev. Solid State Sci., 2 (1988) 115.
4 F. Hanic, I. Horvát and L. Galikova. Thermochim. Acta, 143 (1989) 123.
5 P.K. Gallagher, Thermochim. Acta, 148 (1989) 229.
6 V. Balek and J. Šesták, Thermochim. Acta, 133 (1988) 23.
7 E. Pollert, A. Tříska, V. Cháb and J. Zemek, in M. Frumar, V. Černý and L. Tichý (Eds.), Material Science Monographs, Elsevier, Amsterdam, 1989.
8 G.W. Toop and C.S. Samis, Trans. Metall. Soc. AIME, 224 (1962) 878.
9 K. Zavěta and J. Šesták, in J. Goetz (Ed.), Proc. XI Congress on Glass, Vol. II, p. 339, DT čSTV, Prague, 1977.
10 B.D. Padsalia and P.K. Mehta in A.V. Narlicar (Ed.), Studies of HTS, Vol. 1, Novo Sci., New York, 1989.
11 W.K. Ford, J. Anderson, G.V. Rubenacker, J.E. Drumheller, C. Chen, M. Hong. J. Kwo and S.H. Liow, J. Mater. Sci. 4 (1989) 16; Phys. Rev. B, 1 (1988) 7924.
12 S.L. Qiu, M.W. Ruckman, N. Brookes, P.D. Johnson, J. Chen, C.L. Lim, M. Strougin, B. Sinkovis, J.E. Crow and C.S. Lee, Phys. Rev. B, 37 (1988) 3747.
13 J. Novák, P. Vyhlídka, D. Zemanová, E. Pollert and A. Tříska, Physica C, 157 (1989) 346.
14 J. Šesták, Z. Strnad and Ž.D. Živkovič, Min. Metall. Q. (Ljublana), 35 (1988) 43 (in Jugoslavian).
15 J. Šesták, Thermochim. Acta, 148 (1989) 235.
16 K. Char, R.W. Barton, A.F. Marschal and A. Kapitulnik, Physica C, 152 (1988) 475.
17 P. Bordet, C. Cheillont, J. Chenavas, J.L. Hodeau, M. Marezio, J. Karpinski and E. Keldis, Nature, London, 334 (1988) 596.
18 E. Pollert, J. Hejtmánek, K. Jurek, J. Kamarád, A. Tříska and D. Zemanová, Cryst. Res. Tech., 23 (1988) K6.
19 J. Kamarád, Z. Arnold and E. Pollert, Phys. Status Solidi B, 144 (1987) K39.
20 M.R. Dietrich, W.H. Fietz, J. Ecke, B. Obst and C. Politis, Z. Phys. B, 66 (1987) 283.
21 J.E. Schirber, B. Morosin and D.S. Ginley, Physica C, 157 (1989) 237.
22 C.W. Chu, P.H. Hor, R.L. Meng, Z.J. Huang and Y.Q. Wang, Phys. Rev. Lett., 58 (1987) 405.
23 H.A. Borges, R. Kwok, J.D. Thompson, G.L. Wells, J.L. Smith, Z. Fisk and D.E. Peterson, Phys. Rev. B, 36 (1987) 2404.
24 M.W. McElfresh, M.B. Maple, K.N. Yang and Z. Fisk, Appl. Phys. A, 45 (1988) 365.
25 M. Kurisu, K. Kumagai, Y. Maeno and T. Fujita, Physica C, 152 (1988) 339.
26 H. Takahashi, Ch. Murayama, S. Yomo, N. Mori, K. Kishio, K. Kitazawa and K. Fueki, Jpn. J. Appl. Phys., 26 (1987) L504.
27 W.H. Fietz, M.R. Dietrich and J. Ecke, Z. Phys. B, 69 (1987) 17.
28 V.P. Glazkov, I.N. Gončarenko and V.A. Somenkov, Solid State Phys., 30 (1988) 3703 (in Russian).
29 J.S. Olsen, S. Steenstrup, I. Johannsen and L. Gerward, Z. Phys. B, 72 (1988) 165.
30 J.J. Capponi, C. Chaillout, A.W. Hewat, P. Lejay, M. Marezio, N. Nguyen, B. Raveau, J.L. Soubeyroux, J.L. Tholence and R. Tournier, Europhys. Lett., 3 (1987) 1301.

31 V. Bayot, C. Dewitte, J.P. Erauw, X. Gonze, M. Lambricht and J.P. Michenaud, Solid State Commun., 64 (1987) 327.
32 C.W. Chu, Z.J. Huang, R.L. Meng, L. Gao and P.H. Hor, Phys. Rev. B, 37 (1988) 9730.
33 R. Griessen, Phys. Rev. B, 36 (1987) 5284.
34 T. Kaneko, H. Yoshida, S. Abe, H. Morita, K. Noto and H. Fujimori, Jpn. J. Appl. Phys., 26 (1987) L1374.
35 M. Cyrot, Solid State Commun., 62 (1987) 821.
36 J. Kamarád, to be published.
37 H. Küpfer, S.M. Green, C. Jiang, Yu. Mei, H.L. Luo, R. Meier-Hirmer and C. Politis, Z. Phys. B, 71 (1988) 63.
38 S. Tamura, S. Takekawa, H. Nozari and A. Umezono, J. Phys. Soc. Jpn., 57 (1988) 2215.
39 S. Han, Yu. Zhang, H. Han and Y. Liu, Physica C, 156 (1988) 113.
40 R.S. Roth, R.J. Dawn, F. Beech, D.J. Whiter and J.O. Anderson, in M.F. Yan (Ed.), Ceramic Superconductors II, American Ceramic Society, Columbus, OH, 1988, p. 13.
41 M. Nevřiva, in A.V. Narlicar (Ed.), Studies of HTS, Vol. 4, Novo Sci., New York, 1990.
42 R.W. Vogel and W. Pocher: Z. Metallkd., 21 (1929) 333.
43 A.M. Gadalla, W.F. Ford and J. White: Trans. Br. Ceram. Soc., 62 (1963) 57.
44 P. Holba, A. Tříska, M. Nevřiva, S. Durčok, L. Matějková and E. Pollert, in M. Frumar, V. Černý and L. Tichý (Eds.), Material Science Monographs, Elsevier, Amsterdam, 1989.
45 M. Nevřiva, E. Pollert, L. Matějkova and A. Tříska, J. Cryst. Growth, 85 (1987) 585.
46 P. Couflant, J.C. Bovin and D. Thomas, J. Solid State Chem., 12 (1976) 133.
47 R. Guilermo, Rev. Chim. Miner., 15 (1987) 153.
48 M. Nevřiva, E. Pollert, J. Šesták, L. Matějkova and A. Tříska, Thermochim. Acta, 136 (1988) 263.
49 K. Oka, N. Nakone, M. Ito, M. Saioto and H. Unoki, Jpn. J. Appl. Phys., 27 (1989) 334.
50 M. Nevřiva, P. Holba, S. Durčok, D. Zemanová, E. Pollert and A. Tříska, Physica C, 157 (1989) 334.
51 T. Aselage and K. Keefer, J. Mater. Res., 3 (1988) 1279.
52 J. Przyluski, K. Borowiec and K. Kolbrecka, in M. Frumar, V. Černý and L. Tichý (Eds.), Material Science Monographs, Elsevier, Amsterdam, 1989.
53 V.A. Fotiev, S.N. Koscheva, V.G. Zubkov, N.A. Paxmeova and V.D. Zhuralev, in N.P. Ljakichev (Ed.), Proc. Phys. Chemistry and Technology of HTS, Nauka, Moscow 1989, p. 51 (in Russian).
54 P.G. Grebeschnikov, G.A. Mikirtischeva, O.G. Schigareva, V.I. Schitova, L.J. Graborenko and S.K. Kuscheva, in N.P. Ljakichev (Ed.), Proc. Phys. Chemistry and Technology of HTS, Nauka, Moscow, 1989, p. 33 (in Russian).
55 R.A. Laudise, L.F. Schneemayer and R.L. Barn, J. Cryst. Growth, 85 (1987) 569.
56 Z. Jishan, J. Xiaoping, H. Jiangua, J. Ming, Y. Yang, Z. Zhiva, G. Yanlong , T. Yajun, Q. Guiwen and H. Zhuangqi, Supercon. Sci. Tech., 1 (1988) 107.
57 H.J. Scheel and F. Licci, Thermochim. Acta, 174 (1991) 115.
58 D.M. De Leeuw, C.A.H.A. Mutsaers, C. Langereis, H.C.A. Smoorenburg and P.J. Rommers, Physica C, 152 (1988) 39.
59 J. Šesták, J. Therm. Anal., in press.